*Advances in Bioceramics and Biotechnologies II.*
Edited by Joanna M. McKittrick and Roger Narayan.


# COMPARATIVE EVALUATION of CRYSTALLIZATION BEHAVIOR, MICRO STRUCTURE PROPERTIES and BIOCOMPATIBILITY of FLUORAPATITE-MULLITE GLASS-CERAMICS

S. Mollazadeh[1], A. Youssefi[2], B. Eftekhari Yekta[1], J. Javadpour[1], T.S. Jafarzadeh[3], M. Mehrju[4] and M.A. Shokrgozar[4]
[1] School of Metallurgy and Materials Engineering, Iran University of Science & Technology, Tehran, Iran
[2] Par-e-Tavous Research Center, Mashhad, Iran
[3] School of Dentistry, Tehran University of Medical Science, Tehran, Iran
[4] National Cell Bank of Iran- Pasteur Institute of Iran

## ABSTRACT

The growing trend for restorative glass-ceramic materials has pushed on to the development of the novel dental glass-ceramic systems. Improved biocompatibility, adequate strength, chemical and wear resistance and excellent aesthetic are the main criteria that make these materials clinically successful. The aim of the present study was to investigate the effect of small additions of $TiO_2$, $ZrO_2$, BaO and extra amounts of silica on the microstructural changes and biological properties of an apatite- mullite base glass-ceramic system. Glass transition temperatures and crystallization behavior were investigated using differential thermal analysis (DTA). Addition of $TiO_2$, $ZrO_2$, BaO and extra amounts of silica to the base glass led to some changes in the crystallization temperatures and morphology of the crystalline phases. DTA results showed that while $TiO_2$ and BaO were effective in decreasing the crystallization temperature of the fluorapatite and mullite crystalline phases, $ZrO_2$ and the extra amounts of $SiO_2$ increased the crystallization temperature. X-ray diffractometry (XRD) and scanning electron microscopy (SEM) revealed that the precipitated crystalline phases were fluorapatite [$Ca_{10}(PO_4)_6F_2$] and mullite [$Al_6Si_2O_{13}$], which apart from the extra bearing $SiO_2$ specimen had rod-like morphology in the other specimens. The rod-like crystalline phases' lengths were small, i.e. <20 μm, in the $TiO_2$ and BaO containing glass-ceramics, but small addition of $ZrO_2$ enhanced the length of crystalline phases to approximately 50 μm. MTT assay was used for cell proliferation assessment. The toxicity of glass-ceramic samples was assessed by seeding the osteosarcoma cells (MG63) on powder extracts for 7, 14 and 28 days. MTT results showed that glass-ceramic samples were almost equivalent concerning their in-vitro biological behavior.

## INTRODUCTION

Fluorapatite ($Ca_5(PO4)_3F$) containing glass-ceramics have attracted attention because of their compatibility with the natural apatite of the human bone and teeth[1,2]. Fluoroapatite is a bioactive compound with an apatite-like structure, in which OH groups have been substituted by fluorine ones. Furthermore, its crystalline structure is more stable than hydroxyapatite, which is an important issue where bioactivity receives attention based on crystalline stability[1-3]. Similarity between hardness of fluorapatite-based glass-ceramics and tooth enamel is another advantage that makes them new candidates for substitution of hydroxyapatite in restorative dentistry[1-3]. In most cases, bulk crystallization is the dominant mechanism of crystallization of needle- like fluorapatite in glass specimens. It is said that using $P_2O_5$ in the glass $SiO_2$-$Al_2O_3$-CaO-$CaF_2$ system leads to the crystallization of fluorapatite and mullite phases[4-9]. In these specimens fluorapatite is responsible to link to the tooth enamel and bone[3] and mullite induces adequate mechanical properties[10]. The latter phase plays a key role in biocompatible glass-ceramics since they are mostly planned to use in the stress bearing areas[2]. Despite of various studies that were performed on the chemical resistance, flexural strength, biocompatibility and phase separation of the apatite-mullite glass-ceramics[4-10], to our knowledge there are few documents about the performance of minor glass ingredients in points of crystallization behavior and biocompatibility properties. The primary purpose of the present study was to gain more insight to the effect of some components like $TiO_2$, $ZrO_2$, and BaO and also additional amount of silica in the mentioned regards.

## MATERIALS and METHODS

The initial glass composition contained $4.5SiO_2$, $3Al_2O_3$, $1.5P_2O_5$, $3CaF_2$, and 2 CaO (mole ratio). Reagent grade chemicals Al $(OH)_3$, $CaF_2$, $TiO_2$, $ZrO_2$, $BaCO_3$, $CaCO_3$, phosphoric

acid, and $SiO_2$ were used as the starting materials in this study. The chemical composition of the prepared glasses, which are coded as G, GS, GZ, GB and GT, are shown in Table 1.

Table 1. The chemical composition of different glasses

| Glasses | G | GS | GZ | GB | GT |
|---|---|---|---|---|---|
| $SiO_2$ | 21.03 | 31.27 | 20.49 | 20.49 | 20.49 |
| $Al_2O_3$ | 35.06 | 30.51 | 34.15 | 34.15 | 34.15 |
| CaO | 8.60 | 7.47 | 8.36 | 8.36 | 8.36 |
| $CaF_2$ | 18.93 | 16.47 | 18.44 | 18.44 | 18.44 |
| $P_2O_5$ | 16.38 | 14.26 | 15.96 | 15.96 | 15.96 |
| $TiO_2$ | ---- | ---- | ---- | ---- | 2.56 |
| BaO | ---- | ---- | ---- | 2.56 | ---- |
| $ZrO_2$ | ---- | ---- | 2.56 | ---- | ---- |

The thoroughly mixed batches were melted in an alumina crucible at 1550°C in an electric furnace for 2 h. Then the molten glasses were cast into a pre-heated steel mold. The resulting glass specimens were cooled naturally to room temperature. Glass transition temperatures and crystallization behavior were investigated using differential thermal analysis (Shimadzu DTG 60 AH). To study the crystallization behavior of the different glasses, the glasses were heat treated from 780°C to 1200°C at a heating rate of 10°C/min for 3 h and then furnace cooled to room temperature. The crystallinity of the specimens was identified by X-ray diffractometry (Jeol JDX-8030 and Siemens-D500). The microstructure of the samples was examined using a scanning electron microscope (Philips – XL 30 and Cambridge – S 360). The samples were etched by 10 wt. % HF solution prior to SEM analysis. MTT assay was used for cell proliferation assessment. The toxicity of glass-ceramic samples was assessed by seeding the

osteosarcoma cells (MG63) on powder extracts for 7, 14 and 28 days. The proliferation and differentiation rates of the osteoblast-like cells were evaluated using extracted powder prepared according to ISO 1993–5 procedure. 0.1 g of powder samples with different compositions were incubated in 1 ml of culture medium. At the end of 7, 14 and 28 days, the mediums were collected for use in different cellular assays. Pure culture medium kept under similar conditions was used as a negative control sample. The proliferation rate of the osteoblast-like cells next to different powder extracts was determined by conducting the MTT (3-[4,5-dimethylthiazol-2-yl]-2,5-diphenyltetrazolium bromide) assay. This test is based on the fact that active cells convert the yellowish MTT to an insoluble purple formazan crystal.

RESULTS and DISCUSSION

Figure 1 depicts the DTA traces of various glasses. The crystallization peak temperatures ($Tp_1$ and $Tp_2$) of different glasses have been summarized in Table 2. Accordingly, there are two distinct crystallization peaks in every one. Besides, the glass transitions ($T_g$) and the crystallization peak temperatures have changed with the addition of the mentioned oxides. Based on these results, while $SiO_2$ and $ZrO_2$ increase the crystallization peak temperatures and their $T_g$, $TiO_2$ and BaO show contradictory trends. This behavior is attributed to rising of the glass viscosity with increasing of $SiO_2$ and $ZrO_2$, through reduction of non-bridging oxygen and /or high ionic field strength of these two oxides[11-15]. A contradictory explanation can be recommended for the effect of barium and titanium oxides, i.e. they increase the numbers of non-bridging oxygen in the glasses and hereby decrease the viscosity of the glasses[16-21]. Figure 2 shows the X-ray diffraction patterns of the glasses after heat treatment at different temperatures. Although it has not been presented here, obtained XRD results indicated that fluoroapatite appears after heat treatment at 780°C only in the glasses GT and GB, probably due to the lower viscosity of these two glasses at this temperature. This phase appears with lower intensities in G, GZ and GS at 870°C. Although the present authors were not able to detect a liquid-liquid phase

separation, crystallization of the fluoroapatite as the first crystalline phase in the $P^{+5}$ and $Ca^{2+}$ rich areas of a liquid-liquid phase separated glass, has been reported previously for the same glass system[4-6].

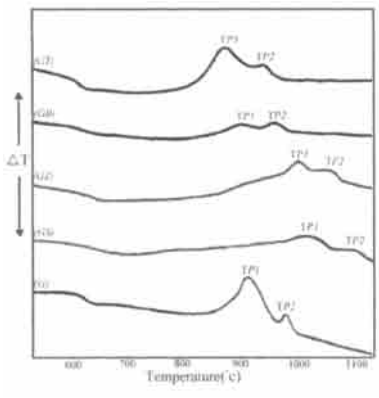


Figure. 1. DTA results of different glass

Table 2. Peak crystallization temperatures

| Glass composition | TP1 | TP2 |
|---|---|---|
| GT | 875 °C | 950 °C |
| GB | 900 °C | 960 °C |
| GZ | 1000 °C | ≈ 1050 °C |
| GS | ≈ 1015 °C | ≈ 1105 °C |
| G | 915 °C | 975 °C |

Mullite precipitates at 870 °C in GT and GB glasses and it is crystallized in GZ and G glasses at 970 °C. Based on the XRD results, apatite and mullite were precipitated in the glasses after the mentioned heat treatment and there was not any footprint of other crystalline compounds, such as $TiO_2$ and $ZrO_2$, in the XRD patterns, meaning that they did not act as a nucleation agent in the glasses. Furthermore, based on the DTA peak crystallization temperatures and the dilatometric softening point temperature of the glasses, it seems that GS has a higher viscosity than GZ. This makes the condition difficult kinetically for the precipitation of the crystalline phases in the GS glass composition and leads to reduction of their XRD peak intensities of the crystalline phases.

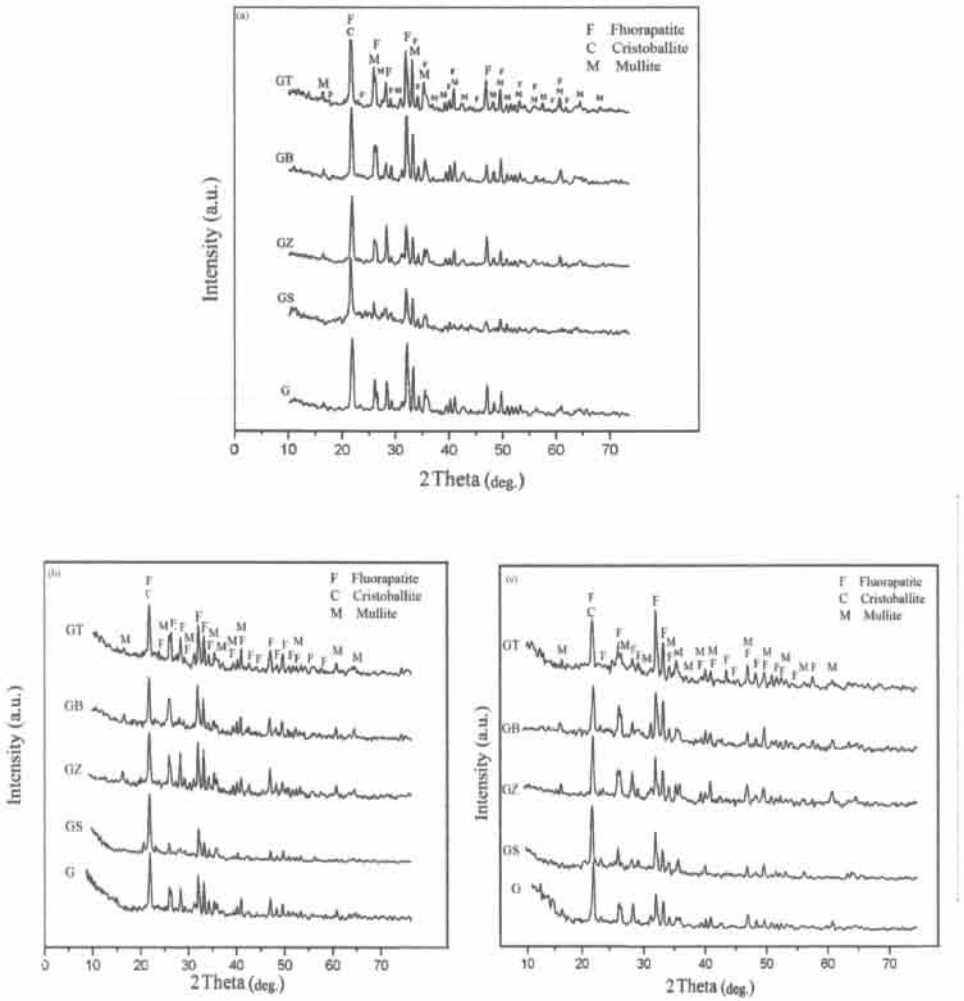


Figure. 2. XRD results of glass compositions heat treated at (a) 1100 °C and (b) 1200 °C for 3hr.

The microstructures of the glasses after heat treatment at 970 °C were investigated. Fig. 3a demonstrates the SEM micrograph of glass G after heat treatment at 970 °C for 3 h.

respectively. This figure shows that heat treatment at 970 °C leads to precipitation of the rod-like crystals of apatite and mullite, with maximum length of about 5 μm. The morphology of crystals changes at 1100 °C. The crystalline particles dissolved in the glassy phase with the increasing of the heat treatment temperature to 1100 °C (pictures have been not presented here). The SEM micrograph of the heat-treated glass GS at 970 °C are shown in Fig. 3b, respectively. Accordingly, the spherical morphology of apatite and mullite crystals is independent of the heat treatment temperature. The microstructures of the glass-ceramics GZ and GB heat treated at 970 °C are shown in Figs. 3c and d, respectively. Based on these figures, the length of rod -like crystalline phases is between 5 -10 μm after heat treatment at 970°C. The crystalline particles kept their morphology even when the specimens were heated at 1100°C. Furthermore, the approximate lengths of crystalline phases increase to about 20 and 50 μm in GB and GZ glass-ceramics, respectively. Fig. 3e shows, the microstructure of glass-ceramic GT. Based on this figure, GT composition has also rod – like microstructure, with a maximum length of about 5 μm. The rod-like particles that according to EDX analysis could be attributed to both fluoroapatite and mullite crystals ultimately start to dissolve in residual glass phase at 1100 ºC. The SEM micrographs of the samples support the XRD results. While apatite and mullite precipitate in the GS as spherical particles in the adopted heat treatment temperature interval, they precipitate in the other glasses as rod-like particles. This difference could be related to the high viscosity of the former glass, due to its higher $SiO_2$ content[21-23]. Spherical fluorapatite particles can also be seen in GT at lower temperatures. Based on the SEM figures, the size of rod shaped crystals in the glass-ceramics GB and GZ are significantly larger than that of G and GT and their aspect ratio has been increased with BaO and $ZrO_2$ addition. The mean lengths of crystals were approximately 20 and 50 μm in glass-ceramics GB and GZ, respectively.

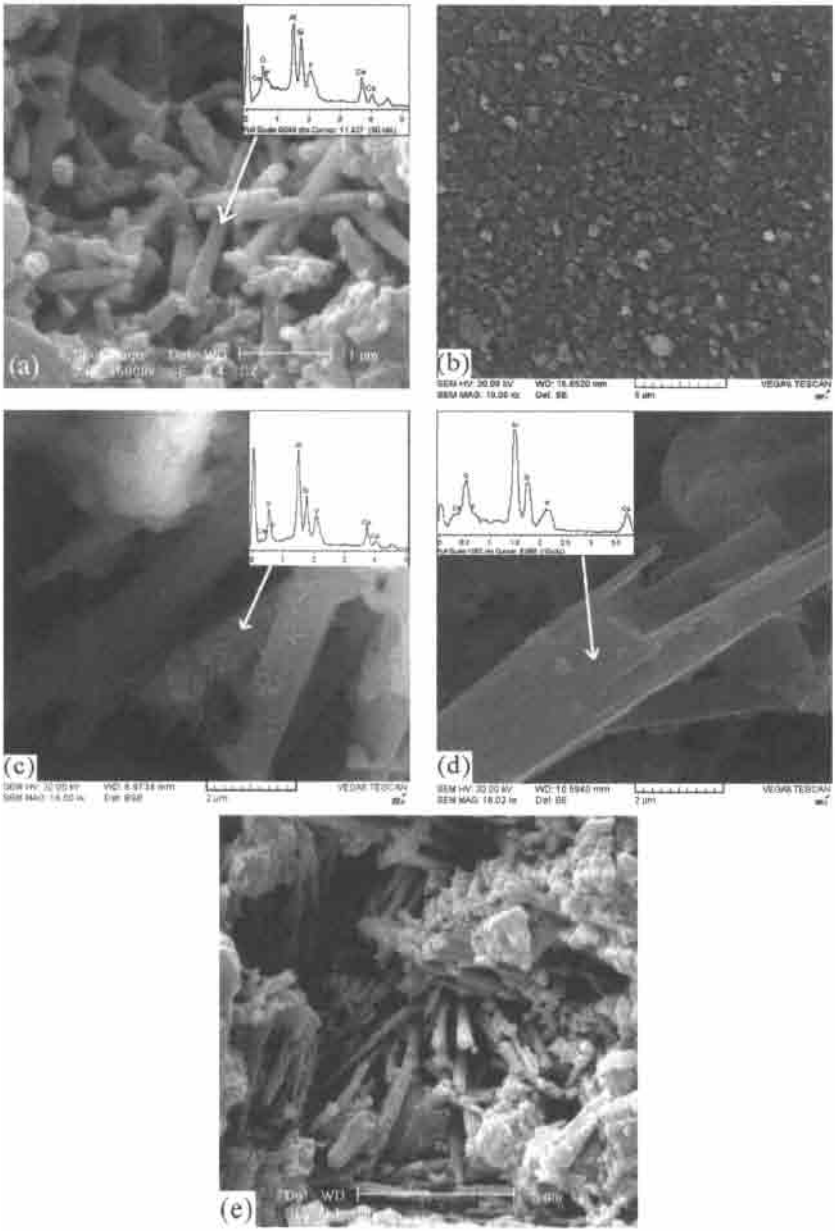


Figure. 3. SEM results of (a) G, (b) GS, (c) GZ, (d) GB and (e) GT compositions heat- treated at 970 °C for 3 h.

Figure 4 represents the results of the percentage cell viability for various powder extracts. MTT results (Fig.4) showed that glass-ceramic samples were almost equivalent concerning their in vitro biological behavior. The MTT results indicate that all of the glass-ceramic samples are biocompatible and the additive oxides and extra amount of $SiO_2$ don not led to the toxicity after 28 days cell proliferation.

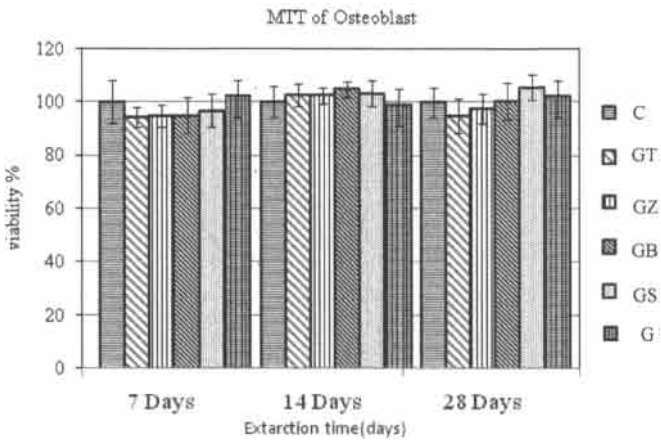


Figure.4. The osteoblast-like cell viability results for various extracted powder samples.

## CONCLUSIONS

Addition of $TiO_2$, BaO, $ZrO_2$ and extra amounts of silica to the base glass led to some changes in the crystallization temperatures and morphology of the crystalline phases. While $TiO_2$ and BaO were effective in decreasing the crystallization temperature of the fluorapatite and mullite crystalline phases, $ZrO_2$ and the extra amounts of $SiO_2$ increased the crystallization temperature. Except for extra silica bearing specimen that showed spherical morphology for both apatite and mullite phases, apatite and mullite precipitated in the other prepared glass-ceramics as rod- like crystals. MTT results showed that glass-ceramic samples were biocompatible. Small addition of additives had a stimulating effect on the cell proliferation.

REFERENCES

[1] C. M. Gorman, R. G. Hill, Heat-pressed ionomer glass-ceramics. Part I: an investigation of flow and microstructure, *Dent. Maters* **19,** 320 –326 (2003).

[2] W. Holland, V. Rheinberger, S. Wegner, M. Frank, Needle – like apatite – leucite glass – ceramic as a base material for the veneering of metal restorations in dentistry, *J. Maters. Sci : Maters in Medicine* **11**, 11 – 17(2000).

[3] L. Montazeri, J. Javadpour, M. A. Shokrgozar, S. Bonakdar, S. Javadian, Hydrothermal synthesis and characterization of hydroxyapatite and fluorhydroxyapatite nano-size powders, *Biomedical Maters* **5,** 1– 8(2010).

[4] K. T. Stanton, R. G. Hill, Crystallisation in apatite-mullite glass–ceramics as a function of fluorine content, *J. Crystal Growth* **275,** e2061–e2068 (2005).

[5] K. Stanton, R. Hill, The role of fluorine in the devitrification of $SiO_2$–$Al_2O_3$–$P_2O_5$–CaO–$CaF_2$ glasses, *J. Maters. Sci* **35**, 1–6 (2000).

[6] M. D. O'Donnell, N. Karpukhina, A.I. Calver, R.V. Law, N. Bubb, A. Stamboulis, R.G. Hill, Real time neutron diffraction and solid state NMR of high strength apatite–mullite glass ceramic, *J. Non-Crys. Solids* **356**, 2693–2698 (2010).

[7] R. Hill, A. Calver, Real-Time nucleation and crystallization studies of a fluorapatite glass–ceramics using small-Angle neutron scattering and neutron diffraction, *J. Am. Ceram. Soc.* **90,** 763–768 (2007).

[8] K. T. Stanton, K. P. O'Flynn, S. Kiernan, J. Menuge, R. Hill, Spherulitic crystallization of apatite–mullite glass-ceramics: Mechanisms of formation and implications for fracture properties, *J. Non-Crys. Solids* **356,** 1802–1813(2010).

[9] A. Clifford, R. Hill, A. Rafferty, P. Mooney, D. Wood, B. Samuneva, S. Matsuya, The influence of calcium to phosphate ratio on the nucleation and crystallization of apatite glass-ceramics, *J. Maters. Sci. Maters in Medicine* **12**, 461– 469 (2001).

[10] C. M. Gormana, R. G. Hill, Heat-pressed ionomer glass–ceramics. Part II. Mechanical property evaluation, *Dent. Maters.* **20**, 252 – 261(2004).

[11] B. Eftekhari Yekta, P. Alizadeh, L. Rezazadeh, Synthesis of glass-ceramic glazes in the ZnO–$Al_2O_3$–$SiO_2$–$ZrO_2$ system, *J. Eur. Ceram. Soc.* **27**, 2311–2315(2007).

[12] M. Rezvani, The effect of complex nucleating agent on the physical and chemical properties of $Li_2O$-$Al_2O_3$-$SiO_2$ glass ceramic, *Iran. J. Mater. Sci. & Engin.* **7**, 8 – 16(2010).

[13] T. Wakasugi, R. Ota, Nucleation behavior of $Na_2O$-$SiO_2$ glasses with small amount of additive, *J. Non-Crys. Solids* **274**, 175–180 (2000).

[14] M. G. Garsia, J. L. Cuevas, C. A. Gutierrez, J. C. Angeles, J. F. Fuentes, Study of a mixed alkaline–earth effect on some properties of glasses of the CaO-MgO-$Al_2O_3$-$SiO_2$ System, *Boletin Sociedad Espanola de Ceramica* **46**, 153–162 (2007).

[15] Y. M. Sung, J. W Ahn, Sintering and crystallization of off-stoichiometric BaO-Al2O3-2SiO2 glasses, *J. Mater. Sci* **35**, 4913 – 4918 (2000).

[16] S. D. Matijasevic,V. D. Zivanovic, M. B. Tosic, S. R.Grujic, J. N. Stojanovic, J. D. Nikolic, S. V. Zdrale, Crystallization behaviour of $Li_2O{\cdot}Nb_2O_5{\cdot}SiO_2$ glass containing TiO2, Process. *Appl. Ceram.* **5**, 223–227(2011).

[17] E. S. Lim, B. S. Kim, J. H. Lee, J. J. Kim, Effect of BaO content on the sintering and physical properties of BaO–$B_2O_3$–$SiO_2$ glasses, *J. Non-Crys. Solids* **352**, 821–826 (2006).

[18] J. E. Shelby, Properties of alkali - alkaline earth metaphosphate glasses, *J. Non-Crys. solids* **263&264**, 271 – 276 (2000).

[19] S. Baghshahi, M.P. Brungs, C. C. Sorrell, H. S. Kim, Surface crystallization of rare-earth aluminosilicate glasses, *J. Non-Crys. Solids* **290**, 208 – 215(2001).

[20] P. F. Becher, M. J. Lance, M. K. Ferber, M. J. Hoffmann, R. L. Satet, The influence of Mg substitution for Al on the properties of SiMeRE oxynitride glasses, *J. Non-Crys. Solids* **333**, 124–128 (2004).

[21] Y. Zhang, J.D. Santos, Crystallization and microstructure analysis of calcium phosphate-based glass ceramics for biomedical applications, *J. Non-Crys. Solids* **272**, 14 – 21 (2000).

[22] Q. Xiang, Y. Liu, X. Sheng, X. Dan, Preparation of mica-based glass-ceramics with needle-like fluorapatite, *Dent. Maters.* **23**, 251–258 (2007).

[23] C. Moisescu, C. Jana, C. Rüssel, Crystallisation of rod-shaped fluoroapatite from glass melts in the system $SiO_2$–$Al_2O_3$–CaO–$P_2O_5$–$Na_2O$–$K_2O$–$F^-$, *J. Non-Crys. Solids* **248**, 169–175 (1999).